RESPONSE ASSESSMENT OF SMALL-SCALE CONFINED MASONRY BUILDINGS THROUGH SHAKING TABLE TESTS

S.M. Alcocer [(1)], N. Casas [(2)]

[(1)] *Research Professor, Institute of Engineering, UNAM, salcocerm@ii.unam.mx*
[(2)] *Graduate Research Assistant, Institute of Engineering, UNAM, casas.guzik@gmail.com*

Abstract

Confined masonry is the most common building material used for dwelling construction in Mexico. The seismic behavior of confined masonry buildings has been generally satisfactory, particularly in Mexico City. Nevertheless, significant damages have been observed in near-epicentral regions during strong ground shaking. To better understand their seismic behavior, a series of shaking table tests were carried out at the Institute of Engineering's shaking table facility of the National Autonomous University of Mexico. One-story, two-story, and three-story confined masonry specimens were built to half scale under Mexican code regulations. A final 1-to-2.4 scale five-story building was built and tested. The experimental program, test set-up and instrumentation, test results, and comparison among models is discussed.

To assess the global and local behavior, the specimens were instrumented with acceleration, displacement and strain transducers. Non-destructive evaluation methods were applied, as well as a series of earthquake ground motions, characteristic of Mexican subduction events recorded in the epicentral region.

Specimen responses were assessed and compared to expected performance under the 2017 Mexico City Building Code standards for masonry construction and seismic design. From recorded and observed results, resisting mechanisms were identified; the structural capacity of each specimen was assessed in terms of crack patterns, strength, stiffness, energy dissipation, and deformation capacity. Observed and measured response from one-, two-, three-, and five-story buildings are compared and discussed. Results will help in clarifying our understanding of confined masonry structures and will let estimate the lateral shear resistance of walls subjected to bending demands. Likewise, it will allow to improve numerical models and performance-based models.

Keywords: confined masonry; seismic performance; shaking-table testing; masonry code; low-cost housing.

1. Introduction

Confined masonry (CM) is the most common material used for dwelling construction in Mexico and in many Latin American countries. CM consists of load-bearing walls surrounded by small cast-in-place reinforced concrete columns and beams, hereafter referred to as tie-columns (TC) and bond-beams (BB), respectively. TC and BB aim at connecting walls and floor systems to achieve structural integrity, as well as to exert in-plane wall confinement, and thus, increase the wall lateral deformation capacity.

The seismic behavior of low-rise CM buildings has been generally satisfactory, particularly in epicentral regions where seismic demands are the highest. Nevertheless, significant damages have been observed in near-epicentral regions during strong ground shaking when code-required design and details have not been followed. In response to this, performance objectives applicable to confined masonry structures should be assessed, specifically for low-cost and low-rise housing developments (1-6 stories), since these designs are commonly repeated several times and their impact on construction cost is very high.

In the past decades, a comprehensive research program of quasi-static tests of isolated masonry walls and systems of walls to natural scale was carried out in Mexico. Nevertheless, few information is available on the response of three-dimensional confined masonry structures subjected to controlled dynamic excitations, like those applied through shaking tables.

In order to obtain more evidence on the dynamic response of confined masonry, a series of shaking table tests were carried out at UNAM Institute of Engineering´s shaking table facility. The research program involved construction and testing of one-, two-, three-, and five-story confined masonry small-scale specimens following the Mexico City Building Code (MCBC) regulations [1]. Layout and detailing are comparable to typical housing prototypes. A similitude model for ultimate strength was selected as the basis for scaling. To assess the global and local behavior, all specimens were instrumented with acceleration, displacement and strain transducers. Non-destructive evaluation methods were applied. A series of earthquake ground motions, characteristic of Mexican subduction events recorded in the epicentral region, were applied through the shaking table. This paper reports on the response of the one-story [2], two-story [3], three-story [4], and five-story models [5], hereafter referred to as M1, M2, M3 and M5, respectively.

2. Experimental program

2.1 Description of the specimens

The shaking table system at UNAM is capable of controlling five degrees of freedom and operates in frequencies ranging from 0.1 to 50 Hz. Due to the physical characteristics of the table (4.0 x 4.0 m, and maximum weight of specimens of 196 kN), the models were constructed such that materials for both the model and prototype were identical, thus following the concept of simple dynamic similarity [6]. Structures dimensions are shown in Figs. 1 and 2. Mechanical and physical properties of the prototype and model materials are given in Table 1. Three wall systems were built in the direction of the earthquake simulator motion (E-W). Facade walls had door and window openings, whereas the middle wall was solid. In the transverse direction (N-S), three walls were built to uniformly distribute gravity loads among walls, to control possible torsional deformations and to improve out-of-plane specimen stability. Model was symmetrical, and the wall distribution was uniform over the specimen height.

2.2 Materials and construction

The model was built on a steel platform that was bolted to the table. Walls were built with hand-made solid clay bricks confined by reinforced concrete TC and BB. Model clay bricks were especially manufactured in a brick factory in Puebla, Mexico (150 km away from Mexico City). The mortar used to join the units had a specified cube-compression strength of 12.3 MPa. The grading of the sand was scaled down to obtain a maximum size of 2.38 mm (M1, M1, and M3) and 1.98 mm (M5). The mortar joint thickness had a 1-mm tolerance.

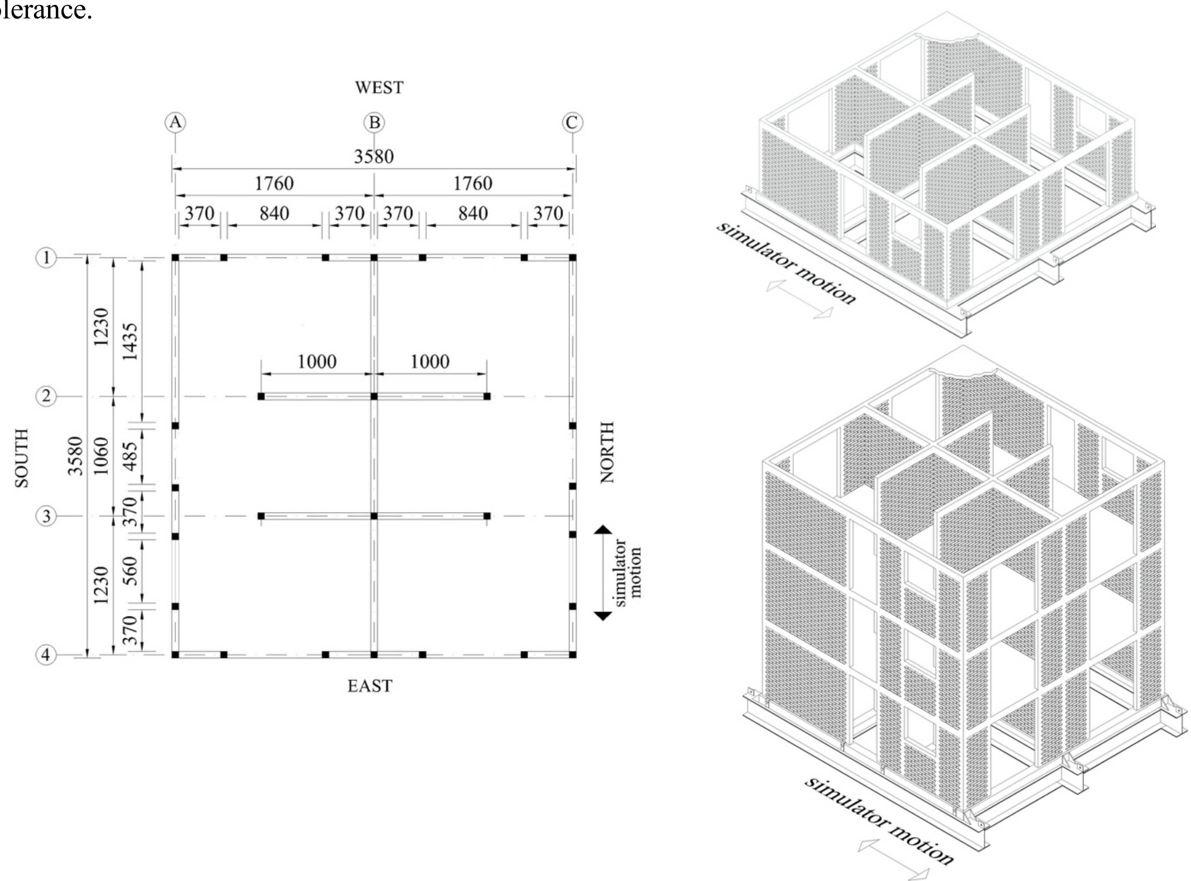

Fig. 1 – Model plan and 3D views of specimens M1 and M3 (units in mm)

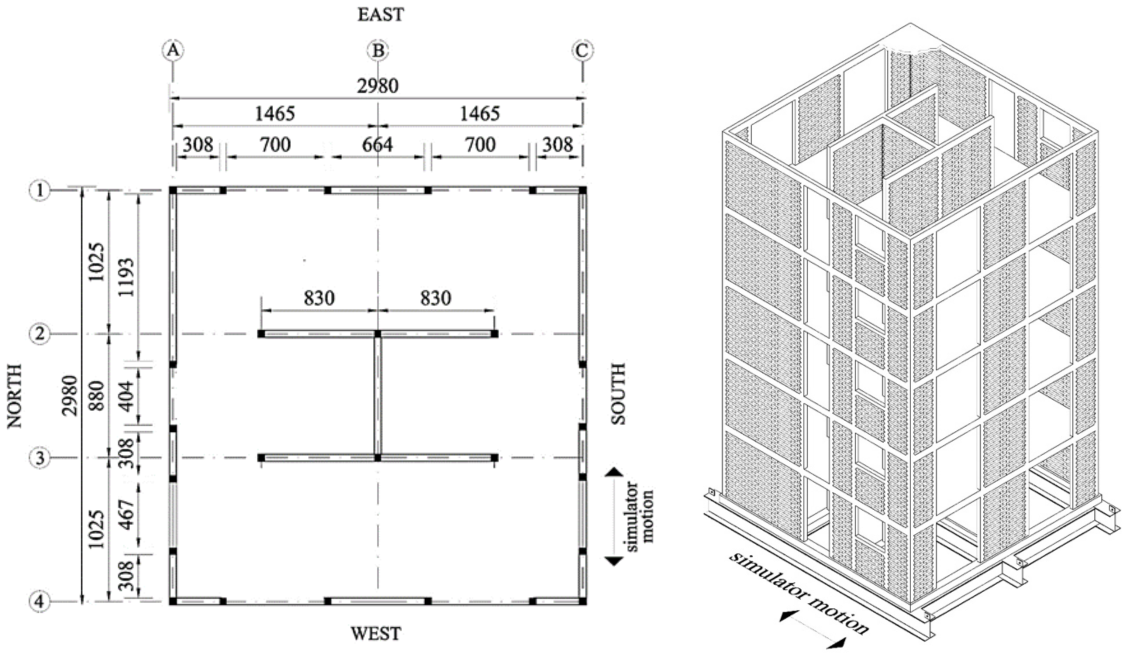

Fig. 2 – Model plan and 3D view of specimen M5 (units in mm)

In TC's concrete, a superplasticizer was used to facilitate concrete placement. Deformed wires were used throughout for the longitudinal reinforcement of TC, BB and slabs, whereas smooth wires were used for hoops. Hoop spacing was reduced at TC's ends to increase TC's concrete confinement and shear strength, control damage and, therefore, to achieve a more stable lateral behavior. Floor systems were cast-in-place reinforced concrete solid slabs, except for the five-story specimen, where prefabricated solid concrete slabs were used for floors 1 to 4, and a cast-in-place reinforced concrete solid slab was used in floor 5, all cast-integrally to BB. Slabs were reinforced with deformed wires in both directions. Reinforcement layout is shown in Figs. 3 and 4. A heat-treatment process was required to adapt the wire stress-strain characteristics to those required by the rules of similarity. Bars were tension-tested and a decrease in yield stress was observed (from 677 MPa to 412 MPa). The stress-strain curve of the heat-treated wires was similar to that of low carbon mild steel reinforcement.

In order to measure the mechanical properties of the materials, small-scale mortar cubes, concrete cylinders, masonry prisms, and square masonry walls, as well as wire coupons, were sampled. Average measured mechanical properties of materials at the time of testing are shown in Table 2.

Table 1 – Physical and Mechanical Characteristics of Prototype and Models

Property, nominal	**Prototype**	**M1, M2 and M3**	**M5**
Area in plan, m^2	51.28	12.82	8.88
Size of door openings, mm	970 x 2170	485 x 1085	404 x 904
Size of window openings, mm	1120 x 1000	560 x 500	467 x 420
Story height, mm	2400	1200	1000
Clay brick size, mm	60 x 120 x 240	30 x 60 x 120	25 x 50 x 100
Mortar joint thickness, mm	10	5	4
TC cross-sectional dimension, mm	120 x 120	60 x 60	50 x 50
BB cross-sectional dimension, mm	230 x 120	115 x 60	96 x 50
Slab thickness, mm	120	60	50
Size of foundation beams, mm	240 x 240	120 x 120	200 x 100
Diameter of longitudinal steel bars, in (mm)	3/8 (9.50)	3/16 (4.75)	5/32 (3.97)
Diameter of steel bars in hoops, in (mm)	1/4 (6.35)	1/8 (3.20)	5/48 (2.65)
Maximum size of aggregate, in (mm)	3/4 (19)	3/8 (9.50)	5/16 (7.94)
Maximum size of sand grain, mm	4.76	2.38	1.98
Nominal strength of concrete, MPa	19.6	19.6	19.6
Nominal strength of mortar, MPa	12.3	12.3	12.3
Nominal yield stress longitudinal steel, MPa	412	412	412
Nominal yield stress of hoops, MPa	245	245	245

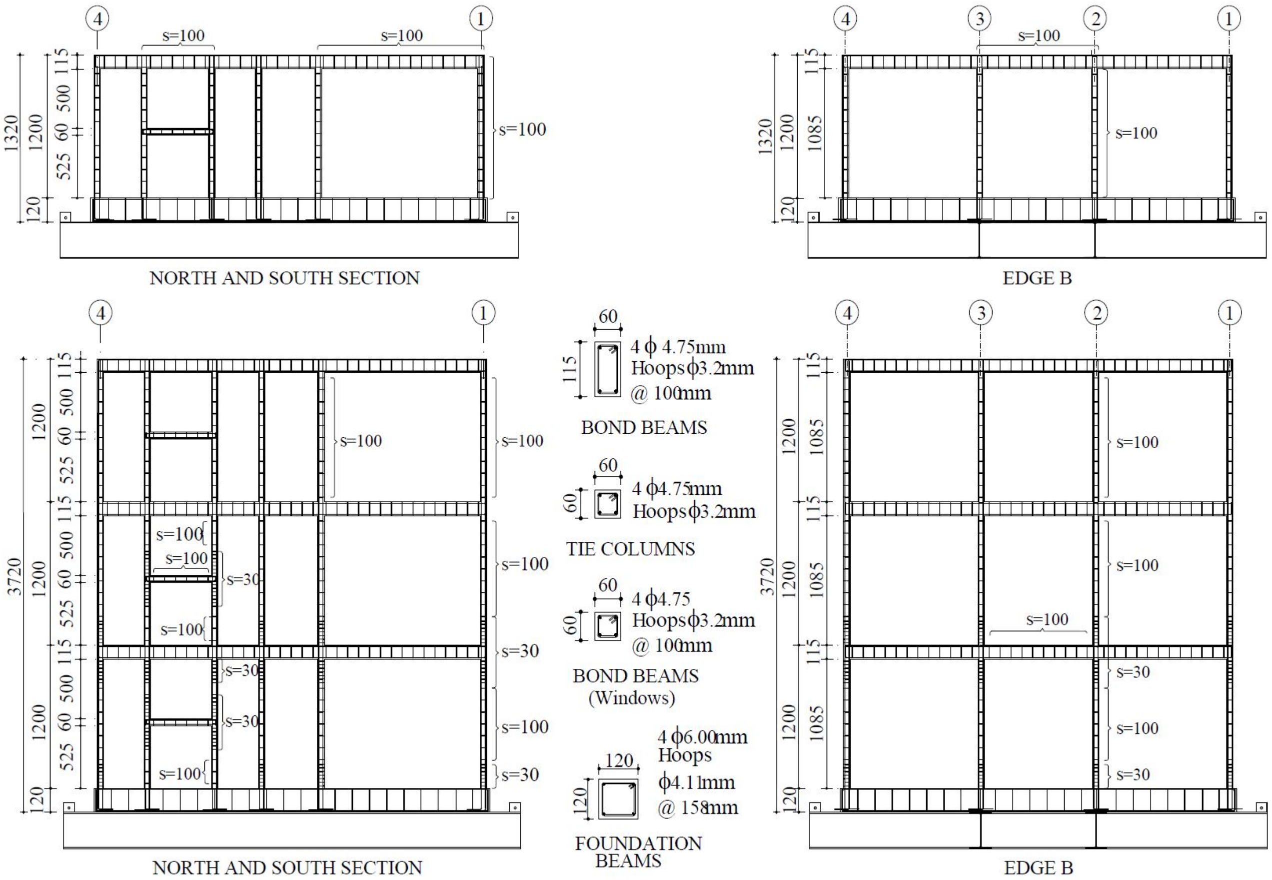

Fig. 3 – Reinforcement layout for specimens M1 and M3 (units in mm)

Table 2 – Mechanical Properties of Materials (MPa)

	M1	M3	M5
Compressive strength of clay brick units	11.8	11.8	5.2
Compressive strength of mortar (cubes)	19.7	16.2	15.7
Compressive strength of masonry (prisms)	7	6.9	3.4
Elastic modulus of masonry (prisms)	1630	1974	1273
Diagonal compression strength of masonry (walls)	1.20	1.18	0.50
Shear modulus of masonry (walls)	1250	807	375.2
Compressive strength of concrete (cylinders)	26.2	21.8	28.4
Elastic modulus of concrete	17801	17009	19580
Yield strength of longitudinal reinforcement	493	493	355
Strength (ultimate stress) of longitudinal reinforcement	584	584	530
Yield strength of hoop reinforcement	269	269	248.5
Strength (ultimate stress) of hoop reinforcement	320	320	396

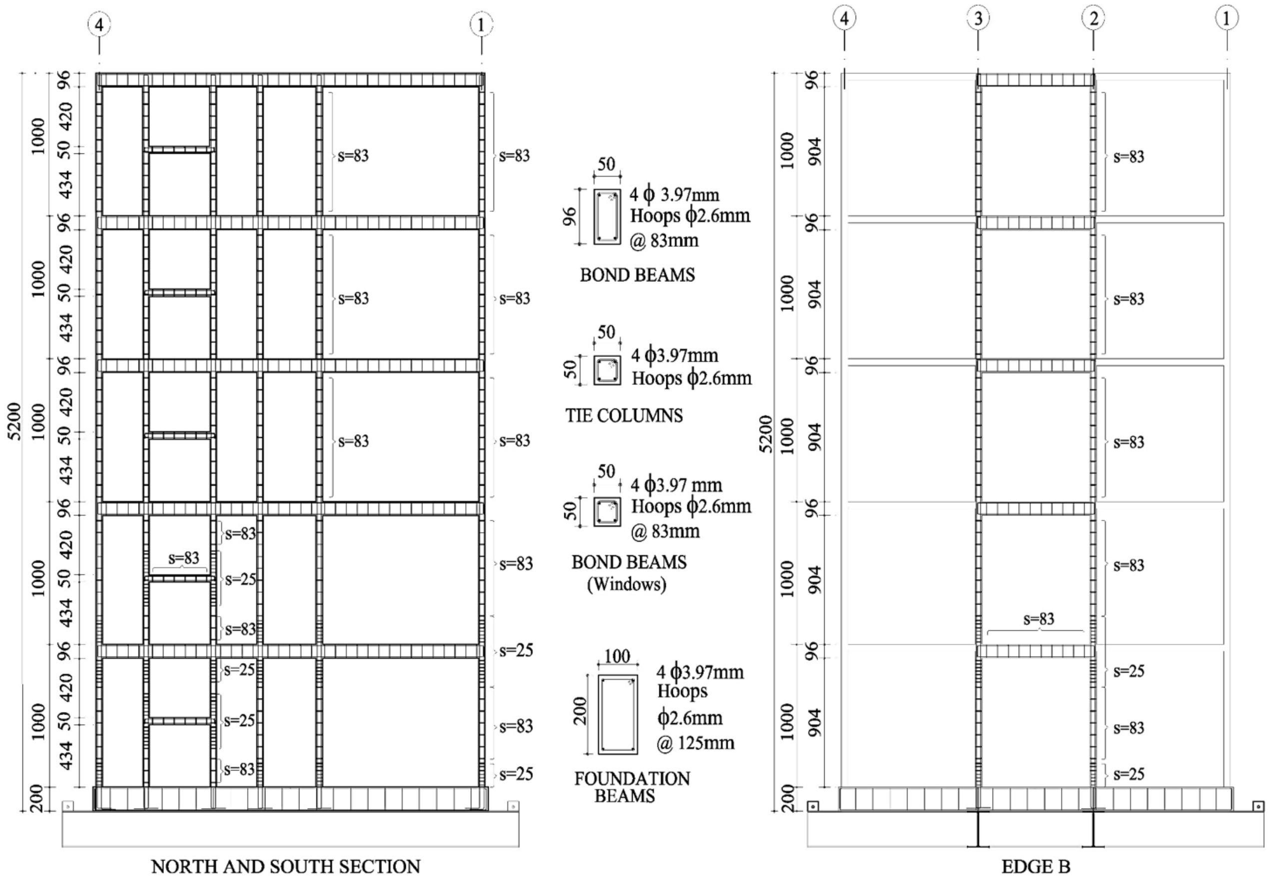

Fig. 4 – Reinforcement layout for specimen M5 (units in mm)

2.3 Instrumentation and test program

To appropriately model the distribution of masses and live loads in the specimens, 0.50-kN lead ingots were attached to floor slabs. Lead ingots were oriented so that their impact on the slab flexural stiffness and strength was minimized. To correctly simulate the vertical stresses on the walls of the prototype, additional prestressing forces were vertically applied onto the walls of the model and were kept constant throughout the testing program. Prestressing forces were applied through small-diameter (3.2 mm) steel strands. Added mass from strands was deemed insignificant.

To assess the global and local behavior, specimen was instrumented with acceleration, displacement and strain transducers. Story displacements, shaking table and story accelerations, wall deformations and reinforcement strains were recorded during the tests.

The small-scaled models were subjected to a sequence of seismic excitations by gradually increasing the intensity of motion at each test run until the final damage state was attained. Between each test run, a random acceleration signal (white noise) at 50 cm/s2 (0.05 g) RMS was applied to identify changes in dynamic properties. For specimens M1, M2 and M3 two earthquake motions, recorded in epicentral regions in Mexico, were used as basis for the testing program. One was the motion recorded in Acapulco, Guerrero, in 1989 (M=6.8). The other was that recorded in Manzanillo, Colima, in 1995 (M=8.0). Both records were considered as Green functions to simulate larger magnitude events. For M5, four earthquake motions were used. One was that recorded in Acapulco, Guerrero in 1989 (DIANA record); a M=7.6 earthquake was simulated considering it as a Green function. The second motion was recorded in Fresnillo de Trujano (FTIG record), Oaxaca in 2017 (M=7.2). The other two motions were recorded at San Juan de los Llanos (SJLL record) in Igualapa, Guerrero in 2012 (M=7.2), and at San Luis de la Loma (SLU record), Guerrero in 2014 (M=7.3). Recorded acceleration and duration were scaled to fulfill the requirements of similarity models.

3. Test results

3.1 Crack patterns

The one-story and three-story models, with their original wall configuration, only suffered minor cracking suggesting elastic behavior. At this stage, the response was characterized by horizontal cracking at the base of the walls. Two walls were removed at edge B, between axis 1-2 and 3-4 (Fig. 1). After wall removal, damage in both specimens was governed by inclined cracking at N and S facades. Simultaneously, horizontal cracks uniformly distributed over the TC's and walls, on the E and W sides, were observed. Slabs also showed cracking perpendicular to the direction of the base motion, attributed to slab bending at the door openings. Analysis of data later confirmed that wall shear deformations controlled the response.

In M1, damage was mainly characterized by horizontal and inclined cracks. The first inclined cracking occurred near the wall center and propagated towards the TC's ends at a drift ratio to 0.30%. Crack propagation into the TC's ends, thus shearing off these elements, was recorded at a drift ratio to 0.67%. At the end of the tests, maximum recorded drift ratio was 1.83%.

In M3, damage was concentrated at the first story (ground floor). Walls exhibited large X-shaped inclined cracks at 45-deg. First diagonal cracks occurred at a drift ratio to 0.23%. Penetration of inclined cracking to TC's ends was recorded at a drift ratio to 0.42%. The maximum recorded drift ratio was 1.71%. A full soft-story mechanism was observed during the test runs. The second story exhibited few horizontal cracks at the base of the walls, whereas in the third story no cracking was observed.

In M5, minor cracking occurred at the base of the walls within the elastic range. At larger intensity motions, damage was governed by wall inclined cracking in N and S facades. Simultaneously, horizontal cracks uniformly distributed over the TC and walls on the E and W sides were observed. Damage was characterized, at the end of the tests, by crushing of the masonry walls, cracking and crushing of TC and by wall inclined crack penetration to TC's ends and kinking of TC's longitudinal reinforcement (thus indicating the development of rebar dowel action). Deep cracks and out-of-plane sliding in square walls of N-S facades were observed. First diagonal cracks occurred at a drift ratio to 0.11%. Penetration of inclined cracking to TC's ends was recorded at a drift ratio to 0.29%. The maximum recorded drift ratio was 0.81%. Final patterns of cracking are shown in Figs. 5 and 6.

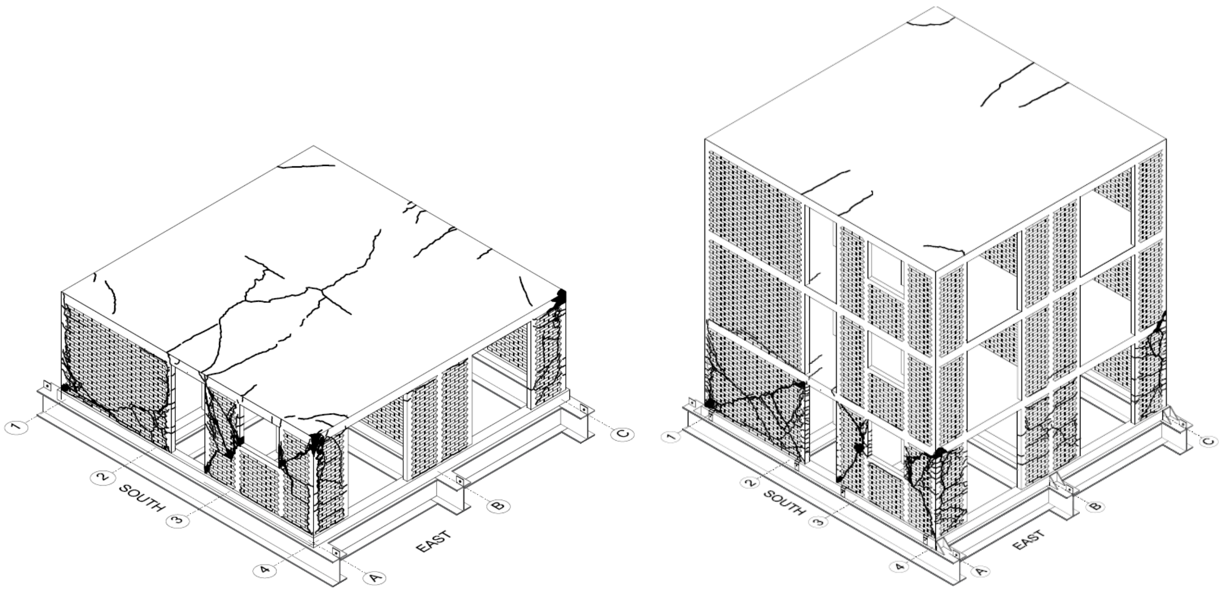

Fig. 5 – Final crack patterns for specimens M1 and M3

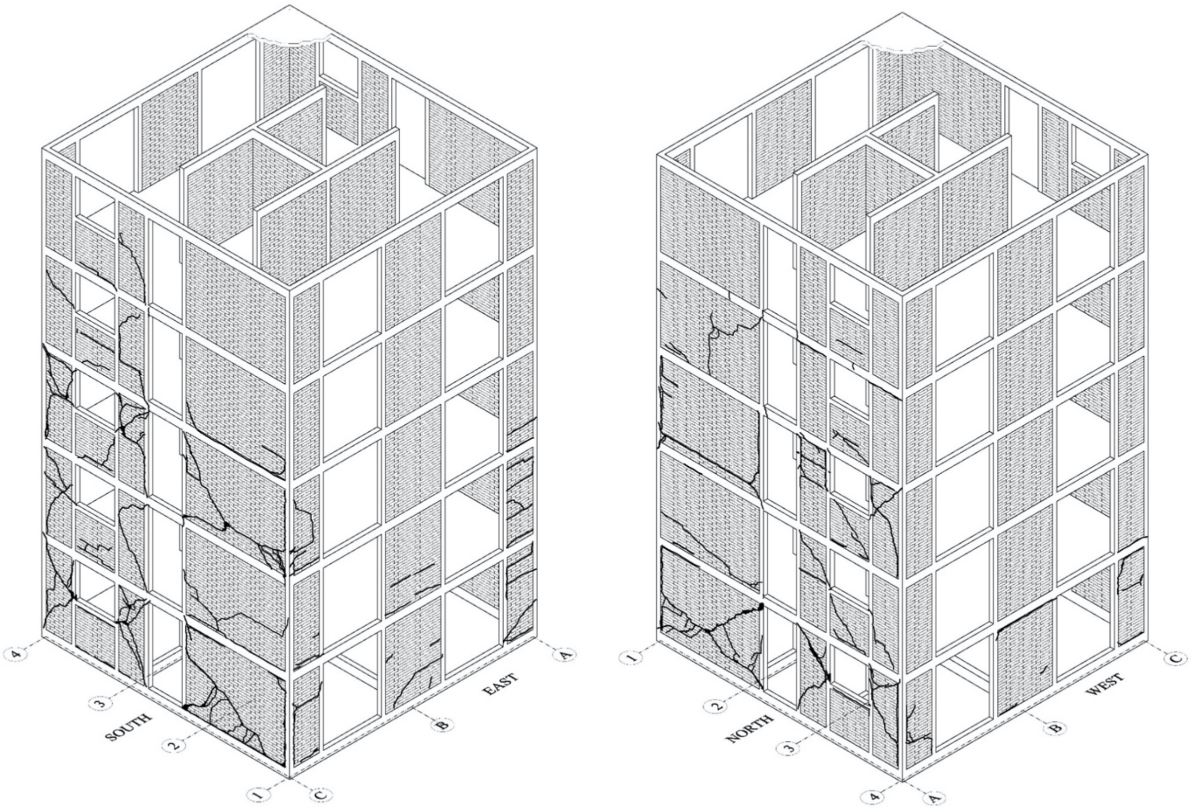

Fig. 6 – Final crack patterns for specimen M5

3.2 Load-deformation curves

To assess the overall performance of structures, the hysteresis curves, in terms of the base shear and lateral drift ratio of the first story, were calculated. The base shear was obtained from the measured accelerations at each floor slab center of gravity and by considering the specimen mass and additional mass from lead ingots. The response envelopes for the specimens are shown in Fig. 7. Also drawn in the response envelope curve, is the strength prediction using the Mexico City Building Code requirements (MCBC, 2004 and 2017). The calculation involved measured material properties at time of testing and as-built wall dimensions. The specimens' overstrength was 2.0, 1.3, and 1.3, for M1, M3, and M5, respectively.

To facilitate comparison among specimens, and among other specimens tested under dynamic or static conditions, three limit states were defined: elastic (E), maximum or strength (M) and ultimate (U). The elastic limit was defined by the occurrence of the first inclined cracking in the masonry wall; strength was achieved when maximum base shear was resisted; and the ultimate limit state was considered at a lateral drift ratio when 20% reduction in strength was recorded.

Hysteresis curves may be found elsewhere [2 to 5]. Specimen M1 showed stable and symmetric loops up to large drift ratios, whereas in M3, hysteresis curves were stable and symmetric up to the strength limit state, after which a severe strength and stiffness decay, because of damage over the walls and at TC's ends, was developed. The second and third stories deformed laterally very slightly, suggesting a rigid body motion over the first story. This phenomenon led to a concentration of deformation and damage at the first story, which performed as a soft-story with a shear-governed mechanism. The hysteresis curves of M5, on the other hand, exhibited instability during the first stages. Damage was concentrated at the first and third floor, although the rest of the stories also exhibited cracking.

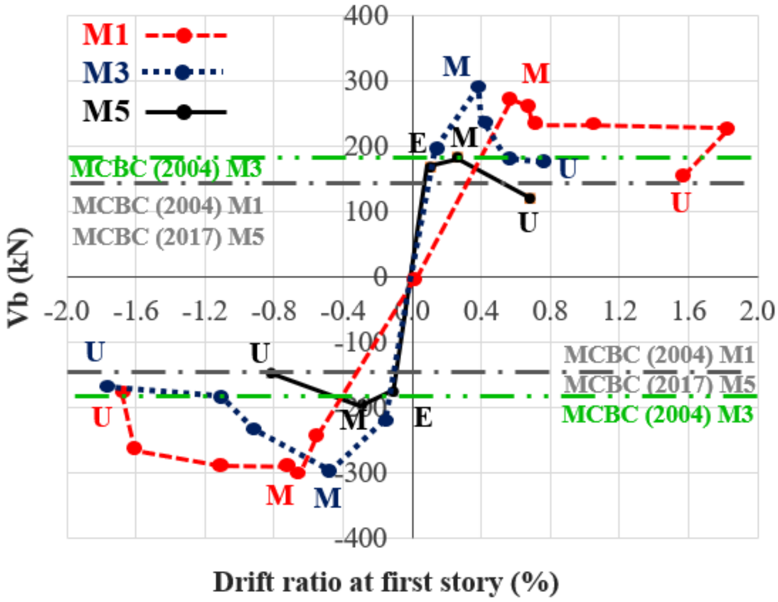

Fig. 7 – Response envelopes for M1, M3, and M5

3.3 Stiffness degradation

Previous test programs aimed at assessing the main characteristics of the hysteretic response of CM structures, have indicated that loss of stiffness is typical even at drift ratios significantly smaller than those at initial inclined masonry cracking. To assess the stiffness degradation phenomenon, peak-to-peak stiffnesses (K_p) were calculated for representative cycles in the models. Normalized stiffnesses are shown in Figure 8. A parabolic decay has been noted so that when first inclined cracking occurs, the remaining stiffness is of the order of 60% of the initial, uncracked stiffness.

Stiffness decay was observed at low drift ratios. This phenomenon is attributed to incipient wall flexural cracking, and perhaps, micro-cracking in masonry materials. After first inclined cracking, the decay increased with drift ratio. At larger drift ratios, K_p remained nearly constant; at this stage stiffness decay is associated to cracking and crushing in masonry walls and reinforced concrete TCs and BBs.

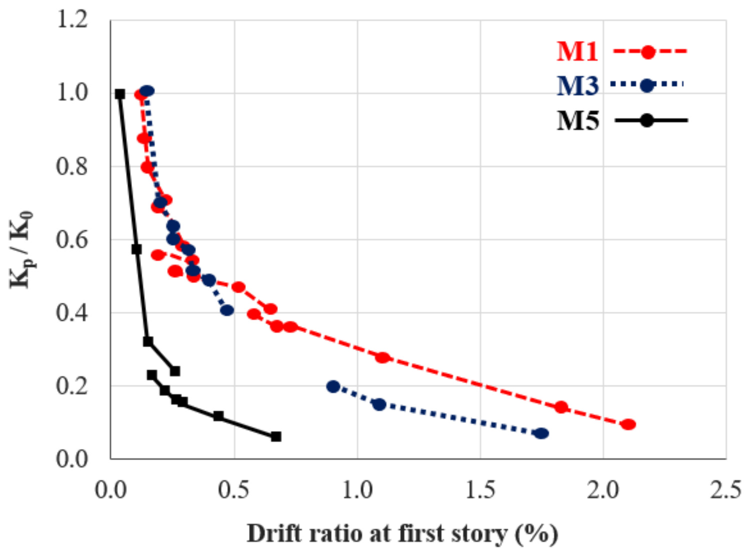

Fig. 8 – Stiffness degradation for M1, M3, and M5

3.4 Energy dissipation

The energy dissipated during the tests was computed as the area within the hysteresis loops from base-shear-to-drift relations. The total cumulative energy dissipated for specimens is shown in Figure 9. Test data show three trends on the curve that correspond to the three limit states (elastic, maximum, ultimate). Before the first inclined cracking occurred, very little energy was dissipated since most of this energy was absorbed by the system through elastic deformations. It is evident that M1 dissipated, in absolute terms, more energy than M3 and M5; moreover, at same drift ratios, M1 also dissipated more energy. It is contended that the failure mode of M1, characterized by shear and sliding mechanisms, contributed to the difference. As for the difference between M3 and M5, it can be attributed to the soft-story mechanism that occurred at first floor in M3, while occurred in the first and third floors in M5.

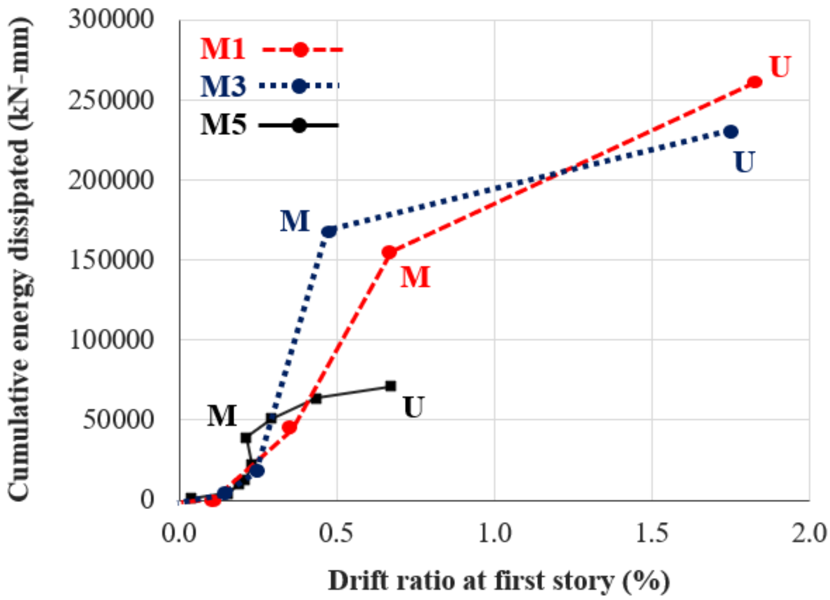

Fig. 9 – Energy dissipated for M1, M3, and M5

3.5 Deformation capacity

Deformation capacity of the model was calculated as the ratio between the ultimate displacement and the yield displacement, expressed in terms of drift ratio at first story. For this purpose, Park's equivalent ductility criterion was used [7]. According to this method, the equivalent ductility is determined from the base shear-to-drift response envelope, considering as ultimate drift the one corresponding to a strength degradation of 20%. The yield drift is obtained from an initial secant stiffness corresponding to 75% of the yield shear, as shown in Figure 10.

The seismic response factor (Q) for CM structures constructed with solid units is specified as Q=2 in the MCBC (2017). Although the seismic coefficient depends not only on the ductility, but also on the hysteretic energy, an approximate way to obtain this parameter from the calculated ductility is through Eq. (1), which is appropriate for short period structures [8].

$$Q = \sqrt{2\mu - 1} \quad (1)$$

Calculated ductility ratios for M1, M2, M3 and M5, are shown in Table 3, for envelopes of positive and negative cycles of the first story. Difference in calculated ductility ratios is attributed to the asymmetric response envelopes for positive and negative cycles, caused by the effect of permanent deformations.

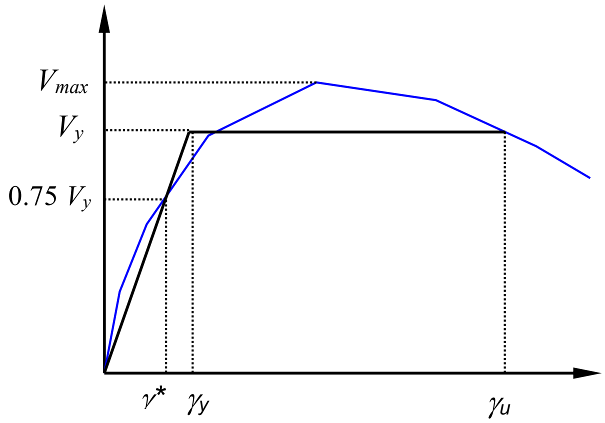

$$\gamma_y = 1{,}33\,\gamma^*$$

$$\mu = \frac{\gamma_u}{\gamma_y}$$

Fig. 10 – Equivalent ductility according to Park's criterion

Table 3 – Equivalent ductility and seismic behavior coefficients

Specimen	cycles	V_y (kN)	γ_u (%)	γ^* (%)	γ_y (%)	μ	Q
M1	(+)	231.73	1.640	0.280	0.370	4.38	2.79
	(-)	251.15	1.620	0.330	0.440	3.67	2.52
M2	(+)	226.53	1.170	0.130	0.170	7.04	3.62
	(-)	257.72	1.300	0.120	0.160	8.13	3.91
M3	(+)	241.24	0.398	0.120	0.160	2.49	2.00
	(-)	250.46	0.750	0.140	0.186	4.03	2.66
M5	(+)	146.05	0.470	0.067	0.089	5.28	3.09
	(-)	156.67	0.700	0.072	0.096	7.29	3.69

4. Conclusions

Conclusions are applicable to CM buildings designed and constructed according to present code regulations from Mexico. Based on the observations made during the tests, it may be concluded that dynamic performance of CM structures clearly indicated that actual design requirements in Mexico are quite safe; actually, are quite conservative. Comparing the calculated and measured strengths, it was found that the level of overstrength of CM structures is of the order of 1.30. Also, it was found that the maximum drift ratio to be allowed for the design of CM structures should be about 0.3% (specimen M5). This value is well below (at 60%) of the drift ratio allowed in the current Mexican standards that is equal to 0.5% [1].

Before specimen M5 was built, the analytical model for design and assessment of CM structures had been simplified by assuming that all the inelastic deformations would take place at the first story (i.e. ground story) and that it would be controlled by shear. However, M5 results showed otherwise, as damage was concentrated on the first and third floor and shear was not the only mechanism that controlled the structure's response. The distinctly different response from M5 is credited to the excitation of higher modes by the earthquake records applied.

By the end of the test, stiffness degradation, obtained from the hysteretic behaviour, was of the order of 90% for all specimens. Measured stiffness degradation followed an exponential decay, where greater degradation was observed at low seismic intensities (drift values under 0.20%) and decreased progressively for higher intensities. This phenomenon is interesting for seismic design methodologies approaches based on performance, since masonry structures can suffer significant stiffness degradation while submitted to small-to-moderate earthquakes.

The drift-cumulative energy dissipated response followed approximately a trilinear curve, coinciding the breaking points with the limit states. Energy dissipated was almost zero before first inclined cracking occurred, however increased at a significant rate afterwards. The highest energy dissipation occurred at final stages where the model exhibited considerable damage.

The deformation capacity of the model estimated with Park's criterion, led to a minimum value of drift ductility at the first story of 4 and a seismic response factor (Q) of 2. This value is comparable with that required in the MCBC (2017) for confined masonry structures, which is adequate if shear deformations concentrated at first story are expected.

5. Acknowledgements

The financial support of the *Instituto para la Seguridad de las Construcciones en el Distrito Federal*, as well as the donations made by *Grupo CEMEX* and *Cementos Moctezuma*, are acknowledged. The participation of the technical staff of the Shaking Table Laboratory at the Institute of Engineering of the National University of Mexico is gratefully acknowledged.

6. References

[1] Mexico City Government (2017): *Normas Técnicas Complementarias*, Gaceta Oficial de la Ciudad de México, No. 220 bis.

[2] Vázquez A (2005): *Ensaye experimental de viviendas de mampostería confinada de un piso mediante el ensaye en mesa vibradora*. UNAM (master's thesis in Civil Engineering), Mexico City, Mexico.

[3] Barragán R (2005): *Ensaye de una vivienda a escala de dos niveles de mampostería confinada*. UNAM (master's thesis in Civil Engineering), Mexico City, Mexico.

[4] Arias G (2005): *Ensayos en mesa vibradora de un modelo a escala 1:2 de un edificio de mampostería confinada de tres niveles*. UNAM (master's thesis in Civil Engineering), Mexico City, Mexico.

[5] Casas N (2019): *Ensaye de un edificio de mampostería confinada de 5 niveles a escala en mesa vibradora*. UNAM (master's thesis in Civil Engineering), Mexico City, Mexico.

[6] Tomazevic M, Velechovsky T (1992): Some aspects of testing small-scale masonry building model on simple earthquake simulator. *Earthquake Engineering & Structural Dynamics*, **21**, 945-63.

[7] Paulay T, Priestley MJN (1992): *Seismic design of reinforced concrete and masonry buildings.* Wiley & Sons, New York, USA.

[8] Newmark N, Hall W (1982): *Earthquake Spectra and Design*. Earthquake Engineering Research Institute, Oakland, USA.